Oral Presentation

The 7th TSME International Conference on Mechanical Engineering
13-16 December 2016

TSME ICOME 2016
Mechanical Engineering Innovation for Green Society

AMM0004

Infrared thermographic non-destructive testing using laser-scanning excitation

Masashi Ishikawa[1,*], Hideo Nishino[1], Masaki Ando[1], Hideyuki Kasano[2] and Hiroshi Hatta[3]

[1] Tokushima University, 2-1 Minamijosanjima-cho, Tokushima, 770-8506, Japan
[2] Nihon University, Nakagawara, Tokusada, Tamura, Koriyama, Fukushima, 963-8642 Japan
[3] Japan Aerospace Exploration Agency, 3-1-1 Yoshinodai, Chuo-ku, Sagamihara, Kanagawa, 252-5210, Japan
[*] Corresponding Author: m.ishikawa@tokushima-u.ac.jp, +81-88-656-7358, +81-88-656-9082

Abstract

In the present study, laser-scanning excitation is examined as a possible heating method for thermographic nondestructive testing. Experimental results for a carbon fiber reinforced plastic specimen with artificial defects showed that the defect detectability of the laser excitation method was comparable to conventional pulse thermography (PT) method, yet it can inspect objects located farther from the heat source than PT. In addition, temperature differences caused by the scanning time delay could be eliminated by using phase images constructed by applying Fourier transforms to temperature-time data. These results suggest that thermographic inspection using laser scanning heating could be an efficient method to inspect large objects located far from observers.

Keywords: Non-destructive testing, Infrared thermography, CFRP

1. Introduction

Active infrared thermography is a convenient method of nondestructive testing because it is a noncontact testing method that can inspect a large area in a short time. Pulse thermography (PT) is a commonly used technique that instantaneously heats test objects using flash lamps and observes the surface temperature distribution after heating [1-3]. If there are some defects inside an object, heat flow from the surface is disturbed by the defects, and an irregular temperature region is observed in the surface. In addition to using the thermal images obtained by the PT, phase images constructed by applying Fourier transforms to the temperature data are also used for nondestructive testing (pulse phase thermography: PPT) [1, 4-6]. It has been reported that the capability of defect detection is higher in the phase images than in the thermal images [7]. In these conventional techniques, heating lamps are located near the test objects in order to provide sufficient heat to generate temperature differences between the defective and nondefective areas. However, because thermographic inspection is a noncontact method, it can also inspect objects located far from the observer if an efficient object heating method is provided.

In this study, we use the laser-scanning excitation method to heat test objects. Because the propagation attenuation of laser energy is significantly smaller than that of conventional optical heating, it can heat objects at greater distances, which allows for remote inspection. In order to achieve remote inspection using laser heating, we start off by investigating the inspection capability of this method experimentally. In Section 2, experiments using laser scanning heating are presented, and the experimental results are compared with the inspection results obtained using conventional PT. In Section 3, inspection for large specimen located farther from the heat source is demonstrated. In addition, when objects are heated by scanning heating, temperature differences caused by the time lag of the scanning is observed in the thermal images, and this becomes a disturbance in defect detection. Thus, a method to eliminate the unwanted temperature difference using phase images is examined in Section 4.

2. Defect detection using laser-scanning excitation

In order to evaluate the defect detectability after laser-scanning heating, experiments on a carbon fiber reinforced plastic (CFRP) specimen were performed. The results were compared with those obtained from the conventional PT method.

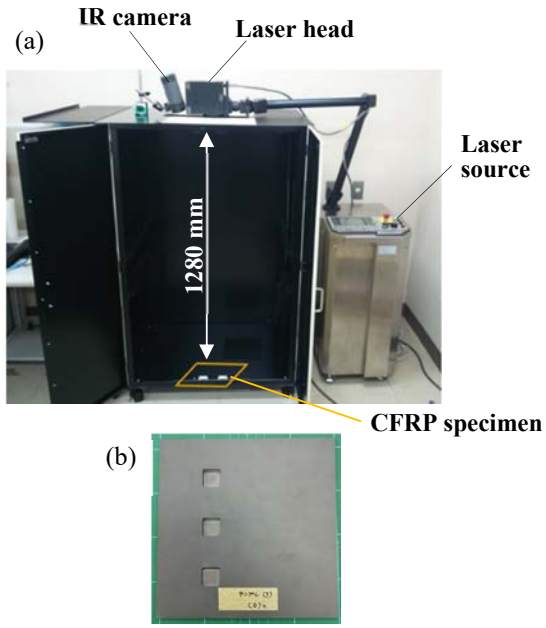

Fig. 1 (a) Thermographic inspection setup using CO_2 laser-scanning system, (b) CFRP specimen with artificial defects.

2.1 Laser-scanning excitation

Figure 1(a) shows a picture of the inspection setup in laser-scanning inspection. A CO_2 laser-scanning system (MultiScan, Rofin-Baasel Inc.) was used to heat the test specimen. The specimen was a unidirectionally reinforced CFRP (200 × 200 × 6 mm) with some square-shaped flat-bottomed holes serving as artificial defects (Fig. 1(b)). The size of the artificial defect was 20 × 20 mm, and the depth from the heated surface varied as 0.5, 1.0, and 2.0 mm. The specimen was located at a distance of 1280 mm from the laser head. The excited laser beam was focused 147 mm away from the lease head, and the beam diameter expanded beyond the focus point. The half width of the laser beam on the surface of the specimen was approximately 45 mm. The scan speed was approximately 750 mm/s, and the excitation energy on the surface of the specimen was 38 kW/m^2. The surface temperature distribution was monitored during and after heating by an infrared (IR) camera (A315, FLIR Systems) with a sampling frequency of 30 Hz.

2.2 Pulse thermography method

Inspection of the same specimen using the PT method was also performed for comparison. In the PT method, two xenon flash lamps (1000 J) were used as the heat source. The lamps were located approximately 30 cm from the CFRP specimen, and the surface temperature was monitored after instantaneous pulse heating with a sampling frequency of 15 Hz.

2.3 Experimental results

Figure 2 shows the thermal images obtained during and after laser-scanning heating (Fig. 2(a) and (b), respectively) and by using PT (Fig. 2(c)). In the images obtained from both the methods, the artificial defects are observed as areas hotter than their surroundings. Figure 3 shows the temperature differences (ΔT) between the defective (defect depth = 1 mm) and nondefective areas as a function of time after heating for both the methods. These results show that the defect detectability using the laser-scanning method is comparable to that using the pulse heating method. However, it is worth noting that the distance between the heat source and tested specimen is larger for the laser excitation method than PT. This means that the laser excitation method can inspect objects located farther than in PT, i.e., it enables remote PT inspection.

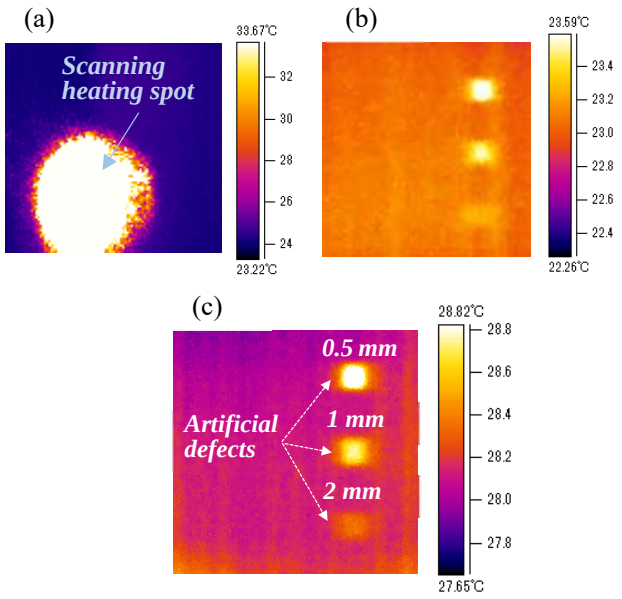

Fig. 2 Thermal images obtained from (a) laser-scanning excitation during heating, (b) laser-scanning excitation after heating, and (c) pulse heating method after heating. Numbers described in (c) show the depth of the artificial defects.

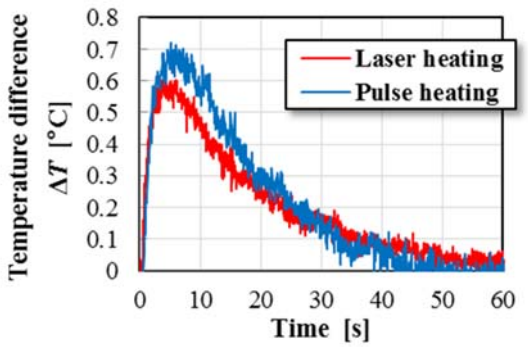

Fig. 3 Comparison of the experimentally obtained temperature difference ΔT between the defective and nondefective areas (defect depth = 1.0 mm) using laser heating and pulse heating methods.

3. Inspection of large specimen using laser-scanning heating

Laser-scanning excitation is considered an efficient method to heat large objects located far from the heat source. In order to examine the inspection capability of defects in large objects, experiments for larger specimen located farther from the laser source were performed.

Figure 4 shows the schematic diagram of a specimen used in the experiments. The specimen was a CFRP laminate with stacking sequence of $[0/90]_n$ with dimensions of 980 × 980 × 6 mm. Square-shaped flat-bottomed holes with three different sizes (20 × 20, 50 × 50, and 100 × 100 mm) were embedded in the specimen as artificial defects. The defect depths from heated surface (t) were 0.5–3.0 mm. Schematic illustration of the experimental setup is presented in Fig. 5. The specimen was placed at a distance of 3 m from the laser head and line-scanned by the CO_2 laser system. The beam diameter on the surface of the specimen was approximately 115 mm, and the beam density was 6 kW/m^2. The scan speed was 450 mm/s in the experiments. The surface temperature during and after heating was observed by the infrared camera with a sampling frequency of 30 Hz. In this experiment, in order to protect the infrared detectors from reflected or leaked laser beams, a partition and a CaF_2 window were

AMM0004

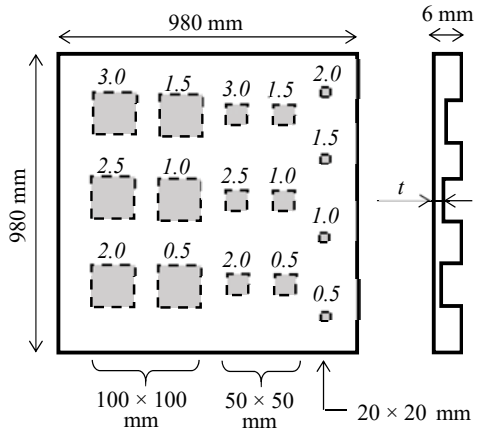

Fig. 4 Schematic diagram of the CFRP specimen used in the experiments in Section 3. Italic numbers described in the figure show depth of artificial defects *t*.

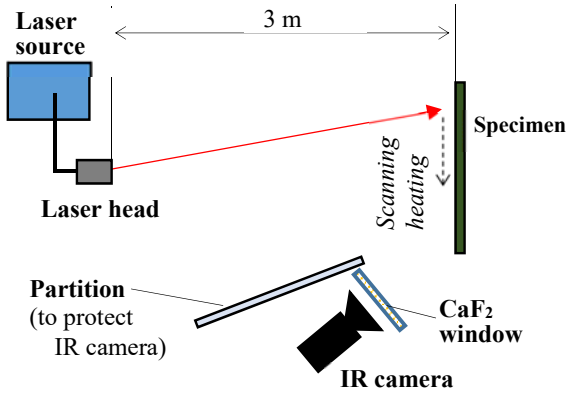

Fig. 5 Setup of experiments for laser heating inspection from a farther distance.

placed beside and in front of the infrared camera, respectively.

An experimentally obtained thermal image after scanning heating is shown in Fig. 6. For both 100 mm and 50 mm size defects, defects at a depth of up to 1.5 mm are detected in the image. Figure 7 shows the temperature difference between defective and nondefective region for 100 mm size defects. The maximum temperature difference for the t = 1.0 mm defect is approximately 0.2°C, which is smaller than the results presented in Fig. 3 (inspection result for small specimen located at approximately 1 m from the laser head). There could be two possible reasons for the decrease in the temperature difference; one is the effect of the CaF_2 window. The transmissivity through the CaF_2 window is approximately 50% when the wavelength is 9.5 µm and it becomes smaller for longer wavelengths. On the other hand, the wavelength detectable by the infrared camera used in the experiments is 7.5–13 µm. Thus, the detected energy was considerably less than that in the previous experiments. Another reason is the decrease of heat input to the specimen. When the diameter of the laser beam, beam density, and scan speed are denoted as d, ρ, and v_l, respectively, the heat input into a certain area Q is calculated as

$$Q = \frac{d\rho}{v_l}. \quad (1)$$

Though the value of Q for the experiments in Section 2 was approximately 2.3 kJ/m^2, the value of Q in this section was approximately 1.5 kJ/m^2. Because the temperature difference is proportional to the heat input, a smaller Q value led to a smaller temperature difference. In other words, the defect detectability could be varied by controlling the laser density and scan speed, regardless of the distance between the laser source and test object.

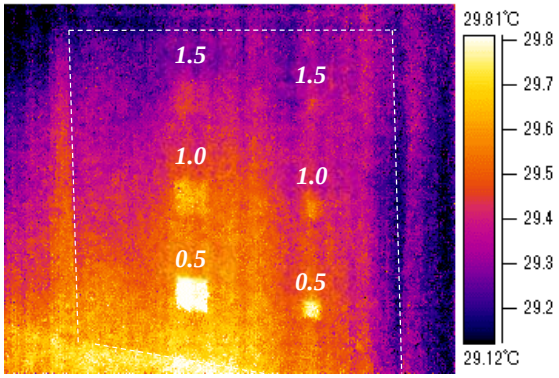

Fig. 6 Experimentally obtained thermal image after laser-scanning heating. Italic numbers show depth of artificial defects.

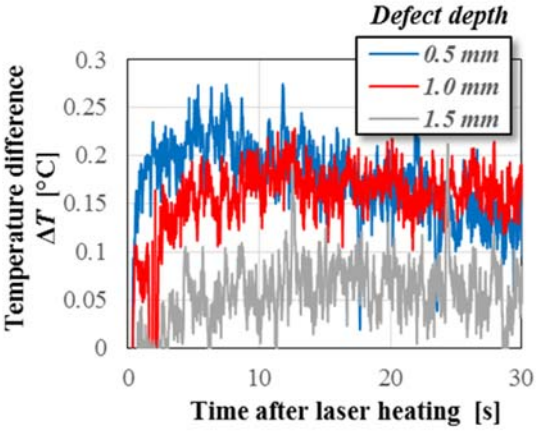

Fig. 7 Temperature difference ΔT between the defective (100 × 100 mm defect) and nondefective regions as a function of elapsed time after heating for a depth of 0.5–1.5 mm.

4. Phase images obtained after scanning heating

Figure 8(a) shows a thermal image obtained after scanning heating the specimen used in Section 2 when the distance between the laser head and the specimen was 580 mm, and Fig. 8(b) shows the temperature profile along the dashed line in Fig. 8(a). As seen in these figures, a temperature gradient is observed from the left side to the right. This temperature gradient is caused by the time lag of scanning heating and could cause a disturbance in detecting defects in the images. In order to eliminate the effect of the temperature gradient, we tried to use phase images constructed by applying Fourier transformation to the thermal data.

When the inspection is performed using conventional flash heating, the method using the phase images is known as the pulse phase thermography (PPT) method. In the PPT method, temperature-time relation obtained by the PT method is Fourier transformed, and phase-frequency relation $\varphi(f)$ is calculated using real and imaginary components (denoted by $R(f)$ and $I(f)$, respectively) obtained by the Fourier transform as

$$\varphi(f) = \tan^{-1}\frac{I(f)}{R(f)}. \qquad (2)$$

By using $\varphi(f)$ for each pixel of the infrared camera, phase images at each frequency are constructed. It is reported that the phase images have an added advantage of eliminating the effect of nonuniform temperature distribution caused by the inspection setup or surface condition of the test object. Thus, it may also be effective in eliminating the effect of temperature gradient caused by scanning heating.

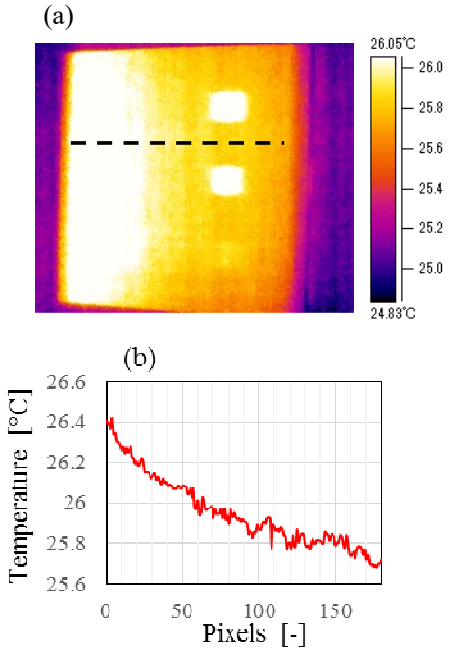

Fig. 8 (a) Thermal image obtained after laser scanning heating (distance between laser head and CFRP specimen is 580 mm), (b) temperature profile along the dashed line denoted in Fig. 8(a).

Figure 9(a) shows the phase image constructed from the thermal data presented in Fig. 8, and Fig. 9(b) is the phase profile along the dashed line. It is found from the figures that the effect of temperature gradient observed in Fig. 8 is eliminated in the phase image. Owing to the elimination of the effect of temperature gradient, the defects were observed more clearly in the phase image than in the thermal image. These results suggest that using phase images proves to be more effective in avoiding the disadvantages of scanning heating and in improving the defect detectability.

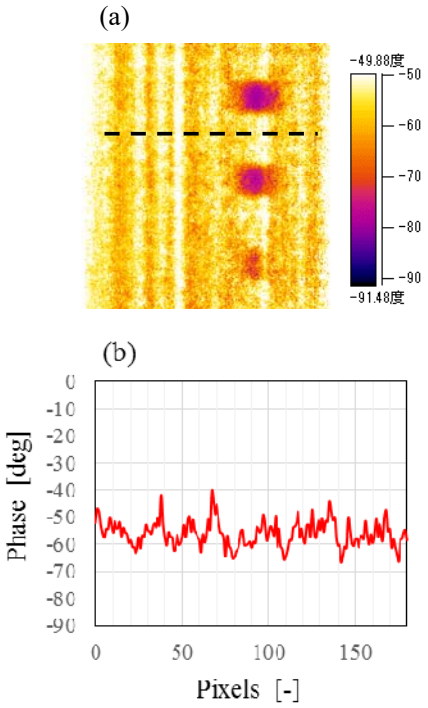

Fig. 9 (a) Phase image transformed from the thermal data presented in Fig. 8, (b) phase profile along the dashed line denoted in Fig. 9(a)

5. Conclusions

The laser scanning heating method was examined in this study with the aim of achieving active thermographic remote nondestructive inspection. Experimental results demonstrated that although the defect detectability observed after laser heating is comparable to that of the conventional pulse thermography (PT) method, the laser heating method could inspect specimens from farther distances than the PT method. These results imply that the thermographic inspection with laser heating could be an effective approach to inspect objects located far away from observers (such as tall bridges or higher parts of large structures). In addition, it was also found that the unwanted temperature gradient caused by the time lag of scanning heating is eliminated by transforming the

thermal images to phase images. Thus, defect detectability of laser scanning inspection can be improved by using phase images.

6. Acknowledgement

This work was supported by JSPS KAKENHI Grant Number 26282099.

7. References

[1] Maldague, X.P.V. (2001). Theory and Practice of Infrared Technology for Nondestructive Testing, John Wiley & Sons, New York.
[2] Sakagami, T. and Kubo, S. (2002). Applications of pulse heating thermography and lock-in thermography to quantitative nondestructive evaluations, *Infrared Physics & Technology*, vol.43(3), June 2002, pp. 211 – 218.
[3] Avdelidis, N.P., Almond, D.P., Dobbinson, A., Hawtin, B.C., Ibarra-Castanedo, C., & Maldague, X. (2004). Aircraft composites assessment by means of transient thermal NDT, *Progress in Aerospace Sciences*, vol.40(3), April 2004, pp. 143 – 162.
[4] Maldague, X. and Marinetti, S. (1996). Pulse phase infrared thermography, *Journal of Applied Physics*, vol.79(5), March 1996, pp. 2694 – 2698.
[5] Maldague, X., Largouet, Y. and Couturier, J. P. (1998). A study of defect depth using neural networks in pulsed phase thermography: modelling, noise, experiments, *Revue générale de thermique*, vol.37(8), September 1998, pp. 704 – 717.
[6] Montanini, R. (2010). Quantitative determination of subsurface defects in a reference specimen made of Plexiglas by means of lock-in and pulse phase infrared thermography, *Infrared Physics & Technology* vol.53(5), September 2010, pp. 363 – 371.
[7] Ishikawa, M., Hatta, H., Habuka, Y., Fukui, R. and Utsunomiya, S. (2013). Detecting deeper defects using pulse phase thermography, *Infrared Physics & Technology*, vol.57, March 2013, pp. 42 – 49.